J Wood Sci (2009) 55:69–73
DOI 10.1007/s10086-008-0997-x

NOTE

Takashi Tanaka · Stavros Avramidis · Satoshi Shida

Evaluation of moisture content distribution in wood by soft X-ray imaging

Received: July 24, 2008 / Accepted: September 5, 2008 / Published online: November 21, 2008

Abstract A technique for nondestructive evaluation of moisture content distribution in Japanese cedar (sugi) during drying using a newly developed soft X-ray digital microscope was investigated. Radial, tangential, and cross-sectional samples measuring 100 × 100 × 10 mm were cut from green sugi wood. Each sample was dried in several steps in an oven and upon completion of each step, the mass was recorded and a soft X-ray image was taken. The relationship between moisture content and the average gray-scale value of the soft X-ray image at each step was linear. In addition, the linear regressions overlapped each other regardless of the sample sections. These results showed that soft X-ray images could accurately estimate the moisture content. Applying this relationship to a small section of each sample, the moisture content distribution was estimated from the image differential between the soft X-ray pictures obtained from the sample in question and the same sample in the oven-dried condition. Moisture content profiles for 10-mm-wide parts at the centers of the samples were also obtained. The shapes of the profiles supported the evaluation method used in this study.

Key words Nondestructive evaluation · Soft X-ray · Moisture content distribution · Drying · Sugi

T. Tanaka (✉) · S. Shida
Biomaterial Sciences Department, Graduate School of Agricultural and Life Sciences, The University of Tokyo, 1-1-1 Yayoi, Bunkyo-ku, Tokyo 113-8657, Japan
Tel. +81-3-5841-5249; Fax +81-3-5684-0299
e-mail: tanakatakash@hotmail.com

S. Avramidis
Department of Wood Science, University of British Columbia, Vancouver, V6T 1Z4, Canada

Part of this work was presented at the 57th Annual Meeting of the Japan Wood Research Society, Hiroshima, August 2007

Introduction

Nondestructive evaluation (NDE) of moisture content distribution is necessary for many wood processes and applications. This is because moisture directly affects processing speed and product quality as well as the physical and mechanical properties along with product behavior in service. NDE methods related to the determination of moisture content are expected to be fast and reliable; thus, considerable effort has been put into this area of research and development over the years.

Various NDE methods to evaluate moisture distribution in wood have been proposed in the past utilizing X-rays, gamma rays, sound waves, microwaves, and neutron beams. X-rays have been used more often and many relevant studies can be found in the literature. Lindgren et al.[1] measured wood density using a medical computerized tomography (CT) scanner and obtained a one-dimensional density profile of Scots pine (*Pinus sylvestris*). For annual rings wider than about 4 mm, it was possible to resolve the detail of the density variation. Wiberg[2] investigated wood density profiles of Scots pine by means of a CT scanner and acquired density and moisture profiles from the green state to about 15% moisture content and he noticed that a very steep moisture gradient developed at the surface during drying. Fromm et al.[3] investigated the water distribution within the sapwood and heartwood of green spruce (*Picea abies*) and oak (*Quercus robur*) as well as in the earlywood and latewood of an annual ring using X-ray computed tomography with a spatial resolution of 0.1225 mm[3]. Tree rings of the sapwood showed steep water gradients from latewood to earlywood, whereas those of the heartwood reflected water deficiency in both species.

In addition to using X-rays, Davis et al.[4] measured moisture content and density of wood distribution of mountain ash (*Eucalyptus regnans*) using a gamma-ray densitometer. They reported that the data agreed extremely well with the independently measured slicing data. Rosenkilde and Glover[5] obtained a one-dimensional moisture content profile in Scots pine from the surface to a depth of 300 μm

during drying using a magnetic resonance imaging (MRI) technique. Simpson[6] measured transit time for sound waves in red oak (*Quercus* spp.) and hard maple (*Acer* spp.) during drying under constant temperature and he established that the speed of sound was sensitive to changes in the moisture content of lumber during drying. Johansson et al.[7] predicted both moisture content and density distribution of Scots pine below the fiber saturation point using microwave scanning in addition to a CT scanner. Nakanishi et al.[8] used a neutron beam and accomplished good imaging of moisture in wood disks 10 mm thick cut from green sugi (*Cryptomeria japonica*). Although the results are promising, all these aforementioned studies still suffer from resolution-related issues, measurable moisture content range level, the size of the measured area, the size of the sample, measuring time, and high cost of equipment.

When exposing wood to soft X-rays, their transmission is decreased in proportion to the density and moisture content of wood. It is possible therefore to calculate the moisture content distribution in wood using the differences between images from soft X-ray images obtained from a sample of known moisture content and the same sample in the oven-dried condition. In this study, the moisture content distribution of the entire area of sugi samples ranging from green to oven-dried was evaluated nondestructively and quantitatively using a newly developed soft X-ray digital microscope.

Materials and methods

Each radial, tangential, and cross-sectional sample of sugi measured 100 × 100 × 10 mm and was cut from green wood with an average initial moisture content of about 80% (Fig. 1). Green sample weights were measured using an electronic balance and immediately thereafter, soft X-ray images were taken by a digital X-ray microscope (μB1600, Matsusada Precision, Kusatsu City, Japan) with tube voltage and current of 35 kV and 180 μA, respectively (Fig. 2). The gain was constant. Grayscale brilliance values were converted from the photon numbers detected by a complementary metal oxide semiconductor (CMOS) image sensor. The maximum size of scanned specimen that can be obtained as a soft X-ray image in one shooting was about 11 × 11 mm on the sample stage. However, in this study, one large soft X-ray image as 5112 × 5111 grayscale bit-mapped image file was obtained by tiling 10 × 10 images. Afterward, the samples were placed in a drying chamber at 105°C and their weights were measured after 1, 2, 3, and 24 h (oven-dry condition). Upon completion of each drying step, the samples were removed from the oven and a soft X-ray image of each was taken.

With the assistance of image-processing software (Adobe Photoshop 6.0 J), the areas of the soft X-ray images in which the sample showed up were trimmed and saved as

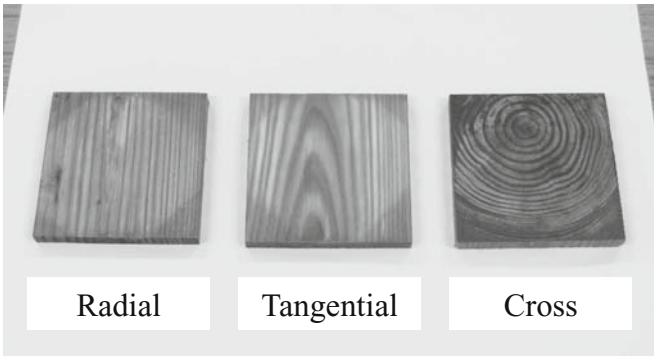

Fig. 1. Wood samples of sugi used in this study

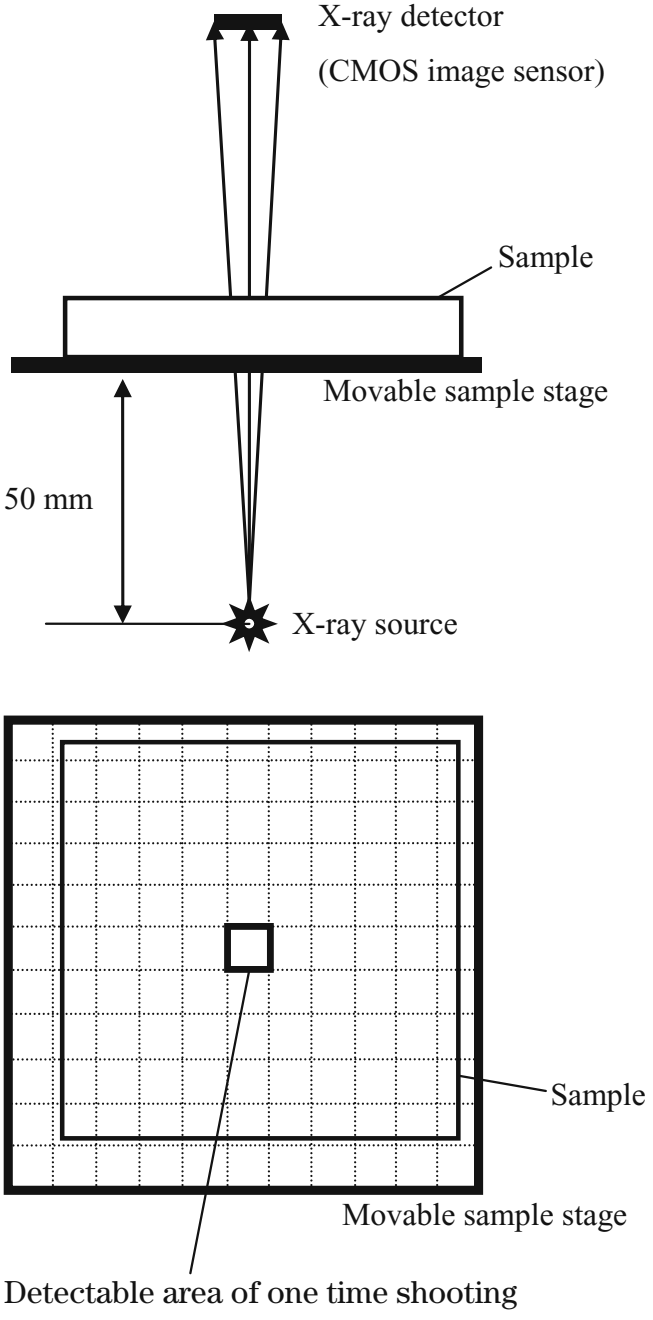

Fig. 2. Configuration of the digital X-ray microscope. *CMOS*, Complementary metal oxide semiconductor

new files; around 4700 × 4700 grayscale bit-mapped images. These sizes depended on drying shrinkage. The grayscale tones of the images were inversed so that where more X-rays were transmitted, the grayscale value became smaller. All images were compacted down to 200 × 200 pixels by means of a bilinear interpolation method and were saved as new files. As a result, these images were equivalent regardless of drying shrinkage, and 1 pixel represented 0.5 × 0.5 mm.

Image differential (Δ_{image}) between the soft X-ray images of the sample with known moisture content and of the same sample in oven-dry condition was obtained by a difference image program (ImgDiff.exe Ver.0.3, Matsusada Precision). Thereafter, it was converted from a bit-mapped format to CSV format to allow further treatment with spreadsheet software.

Results and discussion

Figure 3 shows the relationship between moisture content and the average grayscale values of the soft X-ray images in each sample. It is clear that the average grayscale values of the soft X-ray images decreased after inversion as the moisture content decreased. This was because of the reduction of the mass of water in each sample. Additionally, the plots of the three samples overlapped each other as can also be seen in Fig. 3. Due to this, it was concluded that this relationship is invariable, regardless of sample sections. The linear regression equation and its coefficient of determination (R^2) value of 0.93 indicate that soft X-ray images can accurately estimate the moisture content in sugi specimens.

The relationship shown in Fig. 3 is considered to be applicable to small parts on the samples. For example, given that the samples contained no water after 24 h of oven drying, the water distribution after 1 h of drying is obtained from the grayscale values of Δ_{image} from the soft X-ray images after 1 h and after 24 h of oven drying. Divided by the slope of the regression formula shown on Fig. 3, this grayscale value can be converted to water amount distribution as shown below.

$$wa = \frac{g - g_{\text{oven-dry}}}{a} \cdot W_{\text{oven-dry}} \quad (1)$$

where, wa is the water amount for each point on a soft X-ray image; g is the grayscale value for each point on a soft X-ray image; $g_{\text{oven-dry}}$ is the grayscale value for each point on a soft X-ray image for the oven-dry condition; a is the slope of the regression formula, and $W_{\text{oven-dry}}$ is the weight of sample in the oven-dry condition. Meanwhile, the wood substance amount for each point on a soft X-ray image is obtained from each grayscale value on the soft X-ray image for the oven-dry condition as below.

$$sa = g_{\text{oven-dry}} \cdot \frac{W_{\text{oven-dry}}}{G_{\text{oven-dry}}} \quad (2)$$

where, sa is the wood substance amount for each point on a soft X-ray image; $G_{\text{oven-dry}}$ is the average grayscale value in the oven-dry condition. From Eqs. 1 and 2, the moisture content for each point on the soft X-ray image is obtained as follows

$$m = \frac{wa}{sa} = \frac{g - g_{\text{oven-dry}}}{a \cdot g_{\text{oven-dry}}} \cdot G_{\text{oven-dry}} \quad (3)$$

Figure 4 shows the soft X-ray image of the radial section sample before drying, in the oven-dry condition, and also the Δ_{image} between the two images. From Eq. 3, the estimated moisture content distribution throughout the samples is shown in Fig. 5. The one-dimensional moisture content profiles over time for an area 20 pixels wide and 100 pixels long (areas A, B, C, D, E, and F shown in Fig. 5) are shown in Figs. 6–8. These profiles were obtained by averaging the grayscale values of the 20-pixel-wide areas A, B, C, D, E, and F.

In the radial sample, the moisture content curve for the longitudinal direction profile had a smooth shape. This means that moisture content gradient observed near the drying surface for the longitudinal direction profile was higher than at the center of the longitudinal direction profile. On the other hand, the moisture content curve for the radial direction profile had a jagged shape. This is

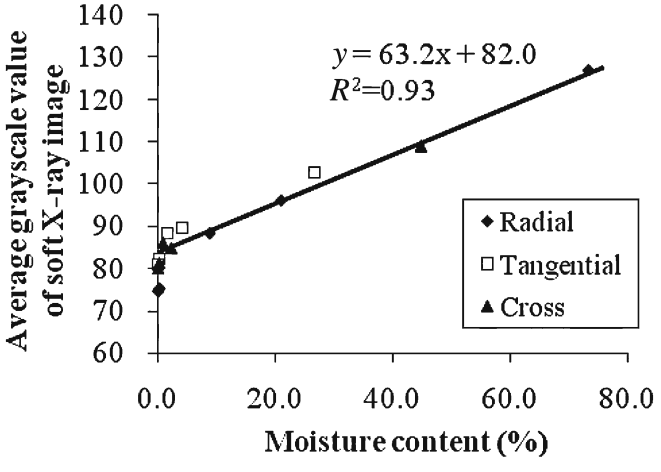

Fig. 3. Relationship between moisture content by oven-dry method and average grayscale value of soft X-ray image

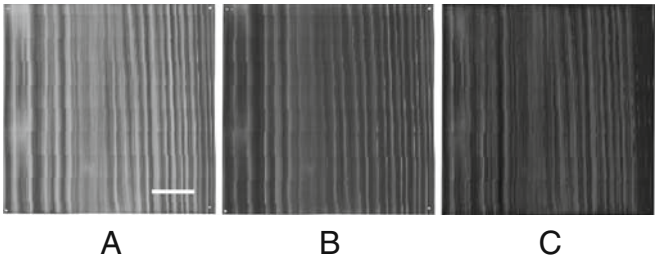

Fig. 4A–C. Soft X-ray images of the radial section sample **A** before drying, **B** after 24 h of oven drying, and **C** the image differential (Δ_{image}). Each pixel becomes whiter as the grayscale value of the pixel increases. *Bar* 20 mm

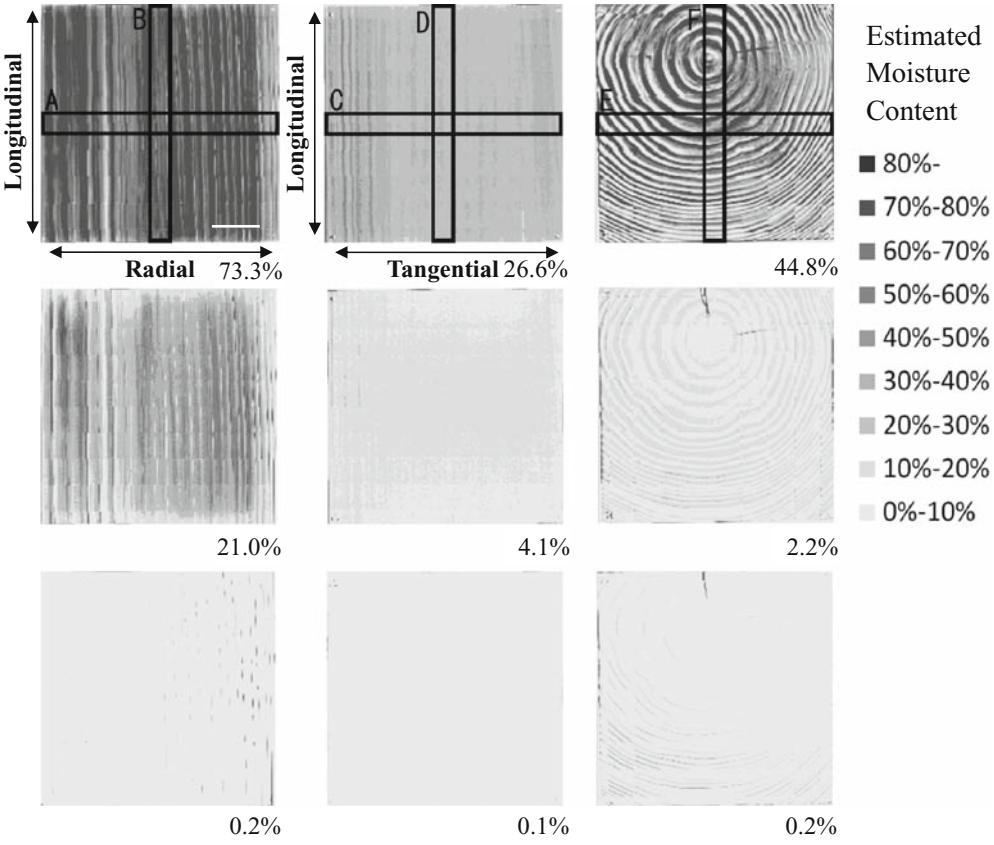

Fig. 5. Images of estimated moisture content distribution during drying. *Left*, radial section sample; *center*, tangential section sample; *right*, images indicate the cross-sectional sample. *Uppermost image*, initial moisture content distribution; *middle image*, moisture content distribution after 1 h; *bottom image*, moisture content distribution after 3 h. *Percentages at bottom right* are the moisture contents measured by oven-dry method. *Bar* 20 mm

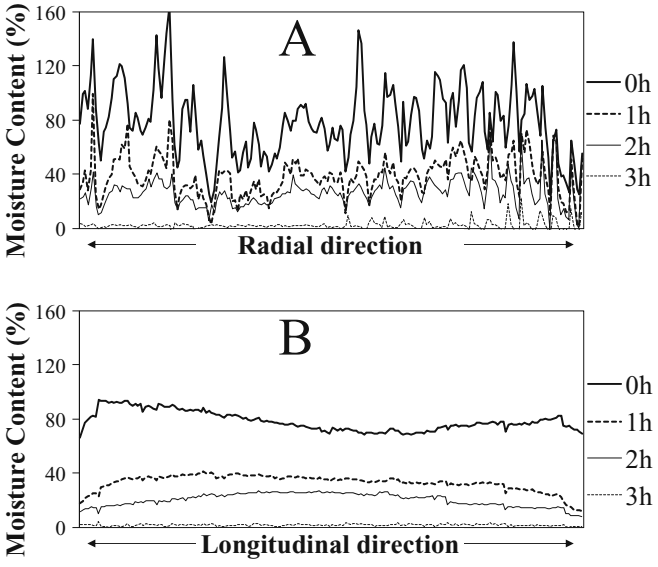

Fig. 6. Changes of moisture content profiles with time for the 10-mm-wide part at the center of the radial section sample, which are the areas *A* and *B* shown in Fig. 5

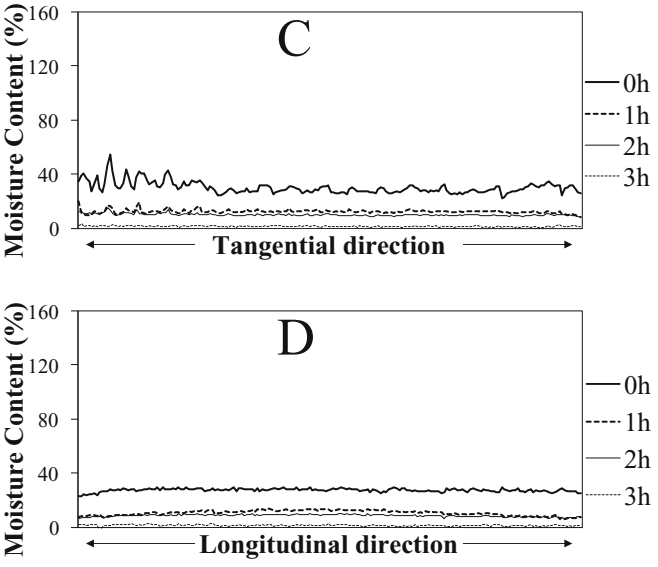

Fig. 7. Changes of moisture content profiles with time for the 10-mm-wide part at the center of the tangential section sample, which are the areas *C* and *D* shown in Fig. 5

thought to be because the flux of water in the radial direction is much lower than in the longitudinal direction. In the tangential section sample, the moisture content curves for the longitudinal and tangential directions were almost flat. This is thought to be because the moisture content gradient is very small in any direction. The reason behind the jagged shape observed on the left end of the moisture content curve for the tangential direction profile is that the section falls between the tangential and radial profiles. In the cross section sample, the drying rate is faster than in any other section. Moisture content in latewood tends to be higher than in earlywood. The above results support the method

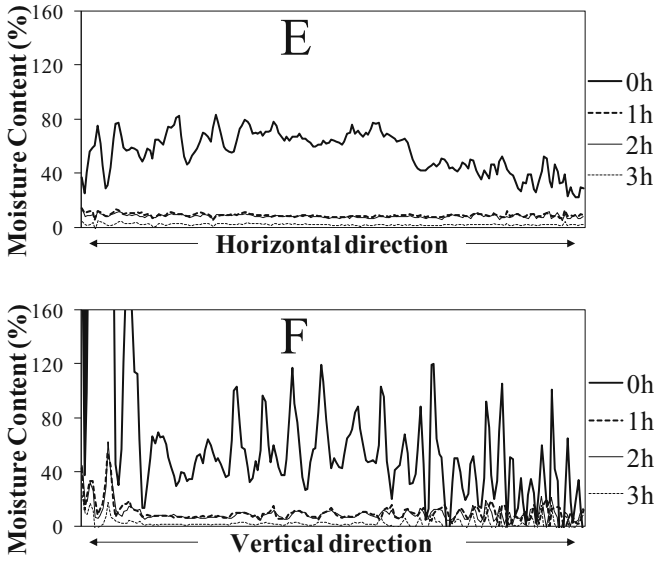

Fig. 8. Changes of moisture content profiles with time for the 10-mm-wide part at the center of the cross section sample, which are the areas *E* and *F* shown in Fig. 5

developed in this study to evaluate moisture content distribution in wood.

It is difficult to determine the moisture content distribution that causes check formation in wood before reaching its oven-dry condition. This is because the positional relationship of the wood substance amount changes after checking; therefore, the wood substance amount, which should be canceled by the Δ_{image}, cannot be canceled. However, in this case, it is still possible to obtain the moisture content distribution from the adjacent wood that exhibits no checking.

The source of X-rays in this study was a point source, which means that the X-rays moved through the sample at an angle that increases with the distance from the center of the X-ray image. Thus, the distance that X-rays penetrate through the sample increases and the decay of the X-ray increases at the extremities of the image. Therefore, the wood substance amount and moisture content level are overestimated at areas far from the center of the X-ray image. The extent of this error varies with the thickness of the sample. This problem might be addressed by reducing the area of the X-ray image. This is a subject of future investigation.

Conclusions

When samples were dried in several steps in a drying chamber and soft X-ray images were taken in each step, the relationship between oven-dry moisture content of each sample and the average grayscale value of the soft X-ray image was linear. In addition, the plots of the three sample types overlapped each other regardless of sample sections. Applying this relationship to a small section of a sample, the moisture content distribution of the entire sample area of 100 × 100 mm was estimated nondestructively from the Δ_{image} from the soft X-ray pictures of the sample in question and the same sample in the oven-dried condition. One-dimensional moisture content profiles for 10-mm-wide parts at the center of the samples were also obtained. The shapes of these profiles supported the proposed evaluation method used in this study. This method can be used for precise analysis of wood–water relations, such as drying mechanism, permeability, and other phenomena.

Acknowledgments This research was partially supported by a Grant-in-Aid for Scientific Research (B) (no. 18380103, 2006) from the Japan Society for the Promotion of Science.

References

1. Lindgren LO, Davis J, Wells P, Shadbolt P (1992) Non-destructive wood density distribution measurements using computed tomography. Holz Roh Werkst 50:295–299
2. Wiberg P (1995) Moisture distribution changes during drying. Holz Roh Werkst 53:402
3. Fromm JH, Sautter I, Matthies E, Kremer J, Schumacher P, Ganter C (2001) Xylem water content and wood density in spruce and oak trees detected by high-resolution computed tomography. Plant Physiol 127:416–425
4. Davis J, Ilic J, Wells P (1993) Moisture content in drying wood using direct scanning gamma-ray densitometry. Wood Fiber Sci 25:153–162
5. Rosenkilde A, Glover P (2002) High resolution measurement of the surface layer moisture content during drying of wood using a novel magnetic resonance imaging technique. Holzforschung 56:312–317
6. Simpson WT (1998) Relationship between speed of sound and moisture content of red oak and hard maple during drying. Wood Fiber Sci 30:405–413
7. Johansson J, Hagman O, Fjellner BA (2003) Predicting moisture content and density distribution of Scots pine by microwave scanning of sawn timber. J Wood Sci 49:312–316
8. Nakanishi TM, Okano T, Karakama I, Ishihara T, Matsubayashi M (1998) Three dimensional imaging of moisture in wood disk by neutron beam during drying process. Holzforschung 52:673–676